

FORMATION OF GUM AND DEPOSITS IN AN OXYGENATED NAPHTHA STREAM

Yonghua Li¹, Paul Watkinson¹
Patricio Herrera², Feridoun Fahiminia², Morgan James²

¹ Department of Chemical and Biological Engineering
The University of British Columbia, 2360 East Mall, Vancouver, B.C., Canada V6T 1Z3
² NOVA Chemicals Research and Technology Centre
NOVA Chemicals Corporation, 2928-16 ST. NE, Calgary, Alberta, Canada T2E 7K7

ABSTRACT

Gums formed when organic fluids are in contact with air can cause fouling of process equipment. The oxidation and formation of gum in a naphtha stream was studied in a stirred batch reactor as a function of temperature (96 to 130°C) and at a total pressure of 584 kPa. Mixtures of air and nitrogen in the pressurizing gas gave dissolved oxygen contents in the range 10-270 ppm wt. Peroxide and existent (dissolved) gum contents were measured over periods of up to 80 hours. Rates of reaction were low, with maximum concentrations of peroxide typically below 4 meq/L, and gum formation rates of 4-5 mg/L-h. Fouling experiments were attempted in a re-circulation loop equipped with either steam or electrically heated annular probes. With bulk temperatures of about 90°C, and test section pressures of 825 kPa, initial surface temperatures from 125°C to 185°C were investigated. At lower surface temperatures, no significant decline in heat transfer coefficient was measured, and deposits were recovered only from the dead zones at the ends of the annular unit after times up to 450h. At higher surface temperatures of 185°C, rapid fouling occurred when dissolved gum content had reached ~2300 mg/L. Gum and deposit analyses were similar, showing oxygen contents of about 20% wt., and carbon contents of 71% wt. Further experimentation is needed to link the gum formation step with the fouling rate.

INTRODUCTION

When organic species such as olefins or other hydrocarbons are in contact with traces of dissolved oxygen, reactions can occur which lead to fouling in process units. Although rigorous exclusion of oxygen or addition of anti-oxidants may eliminate such fouling, in some industrial situations oxygen ingress cannot be easily prevented. An overall picture of chemical reaction fouling from hydrocarbons in the presence of oxygen was given by Taylor and Frankenfeld (1986). Hydroperoxides, the immediate products of reaction of oxygen and hydrocarbons, undergo reactions leading directly to insoluble oxidized species, or in parallel reactions, to dissolved oxidized species which then convert to insolubles. Oxidation products include species such as peroxides, aldehydes, acids, and ketones, as well as components with molecular mass 200-600 g/mol, referred to as gum. The nucleation or agglomeration of the insoluble oxidized

products, may occur in the bulk fluid, or on the surface of the heat exchanger, giving rise to differences in effects of process variables on fouling rates. The chemical mechanisms for such fouling are very complex, nevertheless the generation of fouling precursors can be described by conversion of the hydrocarbon into soluble and insoluble gums. Gum will precipitate from bulk solution when its solubility limit is reached. The limit of gum solubility depends on temperature, the nature of the gum, and the other species in the mixture. The rate of gum formation depends on the composition and structure of reacting species, the dissolved oxygen content, temperature, and the presence of catalysts. The reactions are considered to be free radical reactions which follow the basic autoxidation scheme (Reich and Stivala, 1969).

Wallace (1964) ranks reactivity of hydrocarbons in autoxidation as follows:

Alkyl - aromatics > di - olefins > mono - olefins > paraffins

The naphtha of the present work constitutes essentially 80% saturated alkanes (of which 45% n-alkanes and 55% branched and cyclic alkanes) and 20% aromatics with 11% being benzene and toluene and the rest substituted aromatics. Since there are virtually no olefins present in this naphtha, the alkyl-aromatics and branched paraffins are considered the potential sources of deposits. Literature studies of liquid phase autoxidation of some alkanes are available, however virtually none focus on formation of gums and polymers. Wallace (1964), states that in the n-paraffin series, the ease of oxidation increases as the number of methylene groups increases. N-paraffins are generally of low reactivity, and branched paraffins react much more rapidly, as shown by Mill *et al.*, (1972). Sajus (1968) shows that with initiators, oxidation rates at 60°C for alkenes are a factor of about 20 higher than for the corresponding alkanes. Howard and Ingold (1967) give rate constants for autoxidation of alkyl aromatics. Ethylbenzene is much more reactive than toluene or xylene, and is roughly three times as reactive as n-decane. Benzene itself is relatively unreactive (Bateman *et al.*, 1953).

Taylor (1967) studied deposition during evaporation of air-saturated alkanes. For n-alkanes between C₉ and C₁₆, deposition increased as the carbon number was decreased. Branched paraffins i-C₁₂ and i-C₈ gave roughly double the deposition found with n-C₁₂ and n-C₈. Additions

Table 1. Analysis of Naphtha and Possible Gum Constituents

Class	Component	Typical Molecular Formula	% Component	Typical Gum "Monomer"	Atomic O/C	Atomic H/C
Alkanes	Normal alkanes (C ₄ to C ₁₁)	C ₈ H ₁₈	35.4	C ₈ H ₁₇ O ₂	0.25	2.13
	Branched and cycloalkanes (C ₅ -C ₉)	C ₇ H ₁₄	44.7	C ₇ H ₁₃ O ₂	0.29	1.86
Aromatics	Benzene	C ₆ H ₆	5.6	C ₆ H ₅ O ₂	0.33	0.83
	Toluene	C ₇ H ₈	5.6	C ₇ H ₇ O ₂	0.29	1.00
	Ethyl-benzene; 1,3-dimethyl-benzene,	C ₈ H ₁₀	5.9	C ₈ H ₉ O ₂	0.25	1.13
	1-ethyl-3-methyl-benzene, 1,2,3-trimethyl-benzene	C ₉ H ₁₂	2.8	C ₉ H ₁₁ O ₂	0.22	1.22

of aromatics and naphthene to n-decane generally resulted in reductions in deposition. When linear olefins were added to alkanes, deposit formation increased linearly with 1-olefin content. For olefins, gum formation and fouling studies have been reported by Asomaning et al. (1997) and for indene by Wilson and Watkinson (1995).

The naphtha stream of interest contains numerous species which can react with dissolved oxygen. Katta *et al.*, (1993), approached this problem using a global model, with unidentified lumped reactants such as "fuel" rather than individual chemical species. The aims of this work are to determine the chemical route leading to fouling, and to quantify the effect of dissolved oxygen and temperature on the thermal fouling rate. For a naphtha stream of composition in Table 1, the expected O/C atomic ratio of the gums would be ~ 0.25, and the expected H/C atomic ratio 1.2 to 2.1, depending on whether the substituted aromatics or the alkanes contributed most to gum formation.

EXPERIMENTAL APPARATUS AND METHODS

Batch Reaction Kinetics

Batch reaction studies utilized a 600 ml (6.35 cm ID) stainless steel stirred tank reactor, equipped with an 1/8 hp variable speed stirrer motor, a 780W heating mantle and a pressure relief valve set at 790 kPa. Liquid temperature was measured by thermocouple at a depth 1.5 cm from the bottom of the reactor. N₂ and air mixtures were sparged into the liquid phase, from which liquid samples were withdrawn for analysis. After loading 500 ml of liquid, the reactor was sparged for 10 minutes at room temperature. The reactor was first pressurized to about 205 kPa using an air-N₂ mixture at a desired ratio, then heated to the reaction temperature (80-130 ± 2°C), after which additional gas mixture was introduced until the system pressure stabilized at 584 kPa. This total pressure was used throughout all the

oxidation experiments. A 50-ml liquid sample was taken after a given reaction time and quickly quenched to room temperature for the hydroperoxide or soluble gum determination. After sampling, the total pressure was re-established by adding air/N₂ mixture. The experiment was stopped after 400 ml of liquid had been sampled.

Hydroperoxide concentration was measured using a modified version of method ASTM E298, 60C. Twenty ml of liquid sample was dissolved in 20 ml glacial acetic acid. Five ml of fresh saturated aqueous sodium iodide solution was added and the mixture equilibrated at 60°C for an hour, and then cooled to room temperature. After additions of 1-2 ml starch solution and 10 ml of distilled water, the sample was titrated against 0.01N sodium thiosulphate. The peroxide number was then calculated as

$$PO_x \text{ (meq/L)} = \frac{1000 \times (0.01/2) \times (\text{volume of } Na_2S_2O_3)}{\text{volume of sample}}$$

To correct the volume of Na₂S₂O₃ for oxidation of iodide by the O₂ from atmosphere, blank measurements using 20ml of n-Heptane were performed in parallel to each duplicate sample. Based on 26 blank measurements, the average correction corresponded to a peroxide number of 0.07 meq/L. A modified ASTM D 381 method "Existent Gum in Fuels by Jet Evaporation" was used for the soluble gum measurement. About 40 mL of liquid sample is heated to 150–170°C in an oven under a constant N₂ flow of 1000 ml/min. to strip out liquid components of the naphtha. The residues at the end of heating (typically after one hour) were weighed as the soluble gum content, mg/L. Both peroxide and gum analyses were done in duplicate.

A thermogravimetric analyzer (TGA, Shimadzu TG-50H) was used to characterize gum residues and deposits. A sample of 3~10 mg was first heated under N₂ atmosphere (UHP grade) to 110°C and held there for 30 min, then

heated to 800°C at a constant heating rate of 20°C/min, and held at that temperature for 30min until evaporation or devolatilization was completed. Air was then introduced to burn off at 800°C any carbonaceous material which resulted from the decomposition of the organic gum compounds. Selected samples of gums and deposits were also analyzed by Pyrolysis-GC/MS, and by elemental analysis.

Thermal Fouling Studies

The fouling experiments were performed using a recirculation loop described previously in Watkinson, 2007. For steam heating, a type 316 SS double pipe vertical annular heating section of 0.73m long was constructed from a 26.6mm ID. outer pipe and a 9.5 mm OD. tube. Saturated steam with maximum pressure up to 515 kPa condensed in downflow within the inner tube. Temperatures of the steam inlet and outlet, cooling water inlet and outlet, liquid tank, and test section liquid inlet and outlet were measured by type K thermocouples. Pressures were measured in the gas phase of the feed tank, and the inlet to the test section. With electrical heating, a 1920W, HTRI-type (Heat Transfer Research Inc.) probe was used, manufactured by Ashland-Drew Chemicals. Heated length was 0.102m and diameter 1.07×10^{-2} m. Four E-type thermocouples embedded below the surface of the wall, 78mm from the entrance of the heated section provided three readings to calculate the average surface temperature, and one for a high temperature safety shut-off. Compressed N₂ and air mixtures were used to maintain the required tank atmosphere and pressure. A port permitted liquid to be sampled during flow circulation. Due to the hazardous nature of the naphtha, a safety control program was developed in conjunction with the data acquisition system.

For each run, 8L of liquid was loaded into the feed tank and then heated to the desired temperature. Compressed air was then sparged into the liquid to reach the desired pressure (e.g., 720 kPa). A preheating period at constant temperature preceded most fouling runs in order to raise the gum concentration without fluid circulation and thus to reduce the experimental run time. As oxygen was consumed, the tank pressure and dissolved oxygen was replenished. The tank pressure was first lowered to ~480 kPa in an attempt to release nitrogen, and then repressurized to 720 kPa with air to provide fresh oxygen to the system. This procedure was implemented every 24h during fouling runs. Tank temperature was controlled using cooling water. From the measured flow and thermal parameters at any time during the fouling experiments, the overall heat transfer coefficient U was calculated as

$$U = \frac{Q/A}{\Delta T} \quad (1)$$

In steam heating, Q is calculated from the enthalpy gain of the naphtha,

$$Q = mC_p(T_1 - T_2) \quad (2)$$

and a log mean temperature difference ($LMTD$) was used in Equation (1)

$$\Delta T = LMTD = \frac{\Delta T_1 - \Delta T_2}{\ln(\Delta T_1 / \Delta T_2)} \quad (3)$$

For operation at constant steam pressure (and hence T_{st}), fouling would result in a decline in Q and U .

In electrical heating, Q is obtained from the electrical voltage and current applied to the probe as

$$Q = V \times I \quad (4)$$

Here Q remains constant with time, and ΔT in Equation (1) is given by $(T_s - T_b)$. For operation at constant Q , fouling is made evident by an increase in T_s , and a decline in U . The fouling resistance, R_f , is defined in both situations by

$$R_f = \frac{1}{U} - \frac{1}{U_0} \quad (5)$$

Blended naphtha had a density at 25°C of 710 kg/m³. Thermal properties were based on those of gasoline.

RESULTS AND DISCUSSION

Peroxides Formation in Batch Oxidation Studies

Experiments were performed at temperatures of 96–130°C using 100% air, at 120°C using mixtures of 11–63% air in N₂. Hydroperoxide concentration in the oxidized blended naphtha was measured during each of the experiments. Soluble gum content was measured at the end of a run, or as a function of reaction time in selected experiments. Figure 1 shows the measured hydroperoxide concentrations vs. reaction time at different temperatures. An induction time was observed at each temperature, and decreased with increasing temperature. For 96°C, 110°C and 120°C, the peroxides increase up to a maximum and then level off or decrease, which is similar to findings of previous research with other substrates (Hess and O'Hare, 1950) which show that under a given O₂ partial pressure the peroxides increase initially and reach a maximum and then decrease, and both the time to reach the maximum, and the maximum value itself, decrease with increasing temperature. Figure 1 illustrates typical features of the autoxidation of single component hydrocarbons by the free radical chain reaction mechanism with the peroxides or hydroperoxides as the reaction intermediates. At 130°C, it was believed that

Table 2 Peroxides Formation Rates at Different Conditions (Total Pressure 584 kPa)

Temperature	Air	Avg. Peroxide Formation Rate	[O ₂] Range	Avg. [O ₂]	Specific Peroxide Formation Rate Per Mol O ₂
°C	%	10 ² ×mmol/L.h	ppm	ppm	10 ³ ×h ⁻¹
96	100	1.78	270-261	265	3.03
110	100	45.8	170-120	130	158
120	100	45.7	90-60	72	287
130	100	34.2	20-2	4	364
120	11	3.50	11-7	9	176
120	32	4.72	33-28	31	68.4
120	63	8.28	65-50	56	66.7

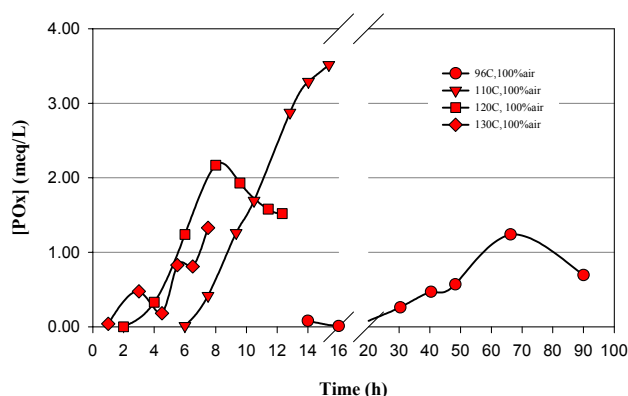


Fig. 1 Effect of Temperature on Peroxides Formation using 100% air at P =584kPa

the peroxides formation was affected by insufficient O₂ supply. Under a constant total pressure, the initial oxygen partial pressure in the vapour phase and dissolved O₂ in the liquid phase decrease with increasing temperature, and the dissolved O₂ decreases during the progress of the oxidation reactions. The dissolved O₂ content for an air-saturated naphtha sample was measured using a GC/MS to be 110 ppmw at 21 kPa and 25°C. The dissolved O₂ concentration over time was then estimated from the measured peroxides concentration and the initial rate of peroxide formation, and the consumption of O₂, assuming the latter to be solely due to the formation of peroxides. Henry's Law and ideal solutions are also assumed. Figure 2 shows the calculated results for experiments at 120°C and 130°C, with 100% air, and the smoothed curves for the both values. Air was added to the system to make up for the pressure decrease which occurred during sampling, leading to the step-wise decrease in calculated dissolved oxygen. The dissolved oxygen content generally decreases due to oxygen consumption and enrichment of nitrogen from the air in the vapour phase. At 130°C, the initial dissolved O₂ (20 ppm) was much lower than that at 120°C (90 ppm), and decreased rapidly due to the reactions, reaching essentially zero after 4.5h. The

effects of dissolved O₂ on peroxides formation were examined at a constant temperature (120°C) with air-N₂ mixtures, covering the range 11% to 100% air. A decrease of the O₂ partial pressure (Figure 3) generally resulted in a decreased peroxides level and a prolonged induction time, with the exception of the data at 11% air. The average initial peroxides formation rate (Table 2) increased linearly with the average dissolved O₂ concentration at low average dissolved O₂ ranging from 10 ppm to about 55 ppm, and then increased markedly at 72 ppm (100% air). This non-linear behaviour may reflect changes in mechanism at low and high dissolved O₂ concentrations (Reich and Stivala, 1969).

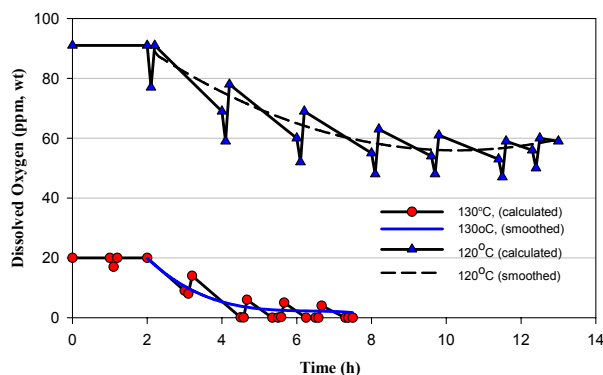


Fig. 2 Calculated liquid phase dissolved oxygen content for T = 120°C and 130°C, and 100% air

Since the peroxide formation rate depends both on temperature and on dissolved O₂ in the liquid, and the data for different temperatures was run at constant pressure (and hence significantly different dissolved oxygen contents), the specific oxidation rate was determined using the average peroxides formation rate determined from the initial slope of the peroxides concentration vs. time curve as shown in Figure 3, and the average dissolved oxygen content (Table 2).

Figure 4 shows the specific peroxides formation rate vs.

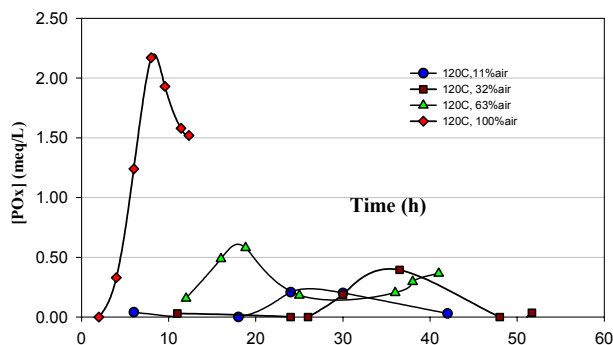


Fig. 3 Peroxides concentrations at 120°C and different air/N₂ mixtures

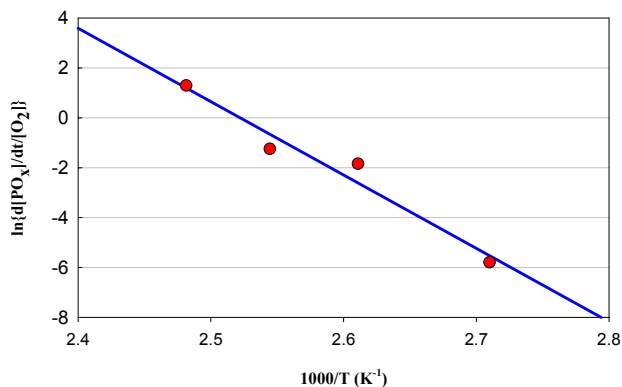


Fig. 4 Specific peroxides formation rates at different temperatures

temperatures as an Arrhenius-type plot with an apparent activation energy of 244 kJ/mol, which corresponds to a doubling of the rate with a 3-4 °C rise in temperature.

Figure 5 shows semi-log plots of $\ln(t_{max})$ and $\ln(t_{in})$ vs $1000/T$, where the induction time at each temperature was determined from the experimental data by extrapolating the linear fitted line of peroxide concentration versus time to the x-axis. The time at which the peroxides formation rate reaches its maximum, t_{max} , is obtained from a simplified model analysis following the basic autoxidation scheme of Reich and Stivala (1969) and assuming a bimolecular decomposition of hydroperoxide in the initial step. Both plots in Figure 5 are parallel to each other and yield a negative apparent activation energy E_a of -78 kJ/mol to -85 kJ/mol from Arrhenius-type equations. The exponential dependence of the induction time as a function of temperature has often been reported for oxidation of single species and some binary mixtures. The magnitude of the apparent activation energy from the t_{max} plot is consistent with expectations from the literature (Reich and Stivala, 1969). Thus, although very complex reactions are involved in naphtha oxidation, the effect of temperature and oxygen

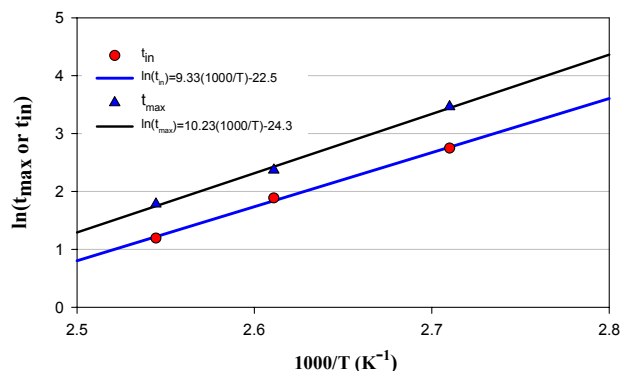


Fig. 5 Logarithm of induction time or time to maximum peroxides formation rate time versus reciprocal of absolute temperature ($1/T$)

content in peroxide formation can be well described by the induction time as measured from the peroxides formation data or by the maximum peroxides formation rate time (t_{max}) from a simple kinetic model analysis.

Soluble Gum and Deposit Formation in Batch Tests

Figure 6 shows the soluble gum contents and the peroxides concentrations measured over time at 120°C with 63% air (oxygen partial pressure of 13 kPa). Both the soluble gum content and peroxide content steadily increase with time. Although the measured peroxides are at a low level, (< 0.5 meq/L up to 43 hours), the soluble gum increased to a steady value of about 210 mg/L. This suggests that the soluble gum may be formed in parallel with the peroxides formation, rather than being a product of subsequent reactions of peroxides.

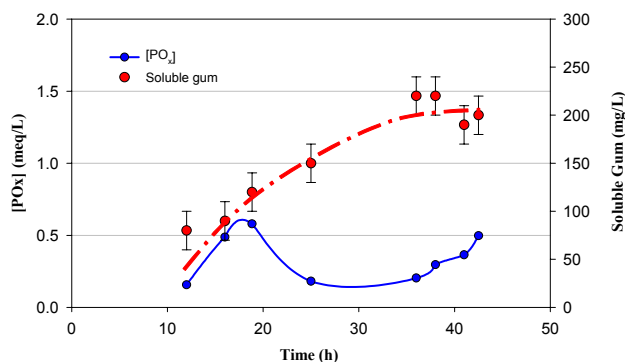


Fig. 6 Gum and peroxide formation in naphtha oxidation (120°C, 63% air)

Figure 7 presents the gum measurements from the bench scale blended naphtha oxidation experiments at 120°C with different air/N₂ mixtures in the atmosphere, for

gum levels below 300 mg/L. One extraneous point (not shown) was found at a concentration above 400 mg/L, after 5h. Although the data are very scattered, gum levels appear to be higher at higher dissolved oxygen contents. Thus increasing oxygen content appears to increase the rate of gum formation, as has been found previously for indene as the single reactive hydrocarbon (Asomaning *et al.*, 1997). On average, the soluble gum formation rate is about 4-5 mg/L-h. Further gum formation data were collected during the subsequent fouling experiments, and will be discussed below.

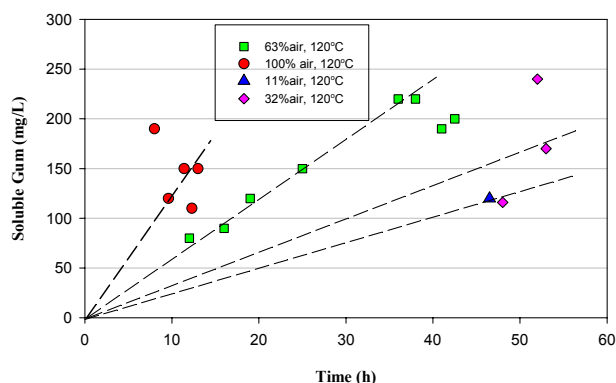


Fig. 7 Soluble gum formation at 120°C and different air/N₂ mixtures

As time increased in the batch experiments, the naphtha changed from colorless to bright yellow. Deposits were found on the reactor interior, corresponding to the liquid level after each sample of liquid was withdrawn. Gum deposits were also collected from the stirrer surface, which was always submerged in the liquid phase. These samples were of sufficient quantity only for TGA analysis, which will be discussed below.

Thermal Fouling Studies

Exploratory naphtha fouling runs were performed (Table 3), each usually at a number of conditions. The soluble gum in the liquid was measured during most of the runs; peroxide measurements were not made. For the steam heating runs, the probe surface temperatures were estimated by a condensation heat transfer calculation for the steam side. Although the steam temperature was generally stable, bulk liquid temperatures at 90°C varied by $\pm 5^\circ\text{C}$ mainly due to the cooling water flow changes. The range of system pressures in Table 3 reflects variations due to the consumption of O₂ by reactions, and periodic purge and repressurization to provide sufficient O₂ for the reactions. Repressurization by sparging air into the holding tank was found to increase U , which affected detection of fouling.

Fouling was not detected in Run 1 which was carried out under relatively mild conditions of 66°C, and surface

temperature to 121°C. For Run 2, a pre-heating period with no circulation was implemented to raise gum levels, and bulk liquid temperature and system pressure were raised. After 147h circulation and heating, when the gum content was 90 mg/L, the liquid sample color had changed to bright yellow. A very thin layer of slightly opaque coating was found on parts of the probe surface; however the heat transfer coefficient was not affected. Brown-colored deposits were found in the stagnant zones at both ends of the heating tube. No measured fouling was evident over the 187 hours (~8 days) of Run 3a, at a surface temperature of 125 °C, therefore for Run 3b: the velocity was reduced to 0.2 m/s, and the steam temperature was increased to 147°C, the maximum attainable, which increased the calculated probe surface temperature to 140°C. Over the eleven days of Run 3b the heat flow and heat transfer coefficient did not decrease measurably, although the liquid became darker yellow with heating time. Brown-colored precipitates appeared on the bottom of sample vials when the initially clear liquid was cooled to room temperature, indicating that the gum followed normal solubility behaviour. As in Run 2, a thin opaque layer coated the probe surface and a brown-black deposit was found on both ends of the probe. The gum content reached 2280 mg/L, after the total run time of 515 h, an average formation rate of 4.5 mg/L-h, which was similar to that found in the isothermal batch tests. Thus in the steam heated runs, in spite of the high gum levels achieved, the thin films which coated the tube surface did not lead to detectable decreases in heat transfer coefficient. However, deposits were found in the dead spaces at the ends of the double pipe exchanger, where some boiling could be expected.

Extended fouling experiments (Table 3) were then performed using the electrical heating probe. In Run 4, two different thermal conditions were used over a total of 480 hours. After preheating with a gum content of 190 mg/L, the heat flow was set at 188W and surface temperature of 160°C. Figures 8 and 9 show the heat flux, surface temperature and heat transfer coefficient plotted versus time. Since significant fouling had not occurred by 300h at a surface temperature of 160°C, the heat flux was increased to 110kW/m² ($Q = 400\text{W}$) through a 30h transition, while other conditions remained unchanged, yielding a surface temperature increase to 185°C. A slow increase of the surface temperature started at about 350h, reaching about 200°C after 40 more hours. At time about 460h a very rapid increase of the surface temperature was observed, in which it rose to 260°C over a 20h period, indicating heavy fouling.

The heat transfer coefficient U increased markedly with the increase on the heat flow at time 300h, typical of sub-cooled flow boiling heat transfer, as has been demonstrated for this type of probe with heptane as the fluid by Muller-

Table 3 Summary of Naphtha Fouling Runs Conditions

Heating Method	Steam Heating					Electrical Heating		
Run	1a	1b	2	3a	3b	4a	4b	5
Pre-heating								
T (°C)	-	-	110	110		110		-
P (kPa)	-	-	585	650		650-720		-
t (h)	-	-	20	70		86		-
Heating								
T _b (°C)	66	66	90-94	90-95	90-95	90	90	90
P _{tk} (kPa)**	585	585	585-650	585-755	585-755	650-720	650-720	650-720
v (m/s)	1.21	0.80	0.79	0.78	0.21	0.32	0.32	0.32
Re	47500	31000	37000	37000	10000	13800	13800	13800
T _s (°C) *	102	121	128	125	140	160	185	165-215
Q (kW)	2.8	2.6	2.0	2.0-2.5	1.0-1.1	0.19	0.40	0.4-1.2
U ₀ (kW/m ² K)	2.01	1.54	1.72	1.8-2.3	0.80-0.96	0.80	0.70-1.22	1.30-2.70
t (h)	8.6	20.8	147	187	260	300	182	805

*calculated for steam heated runs. **Pressure at the test section was some 150 kPa higher

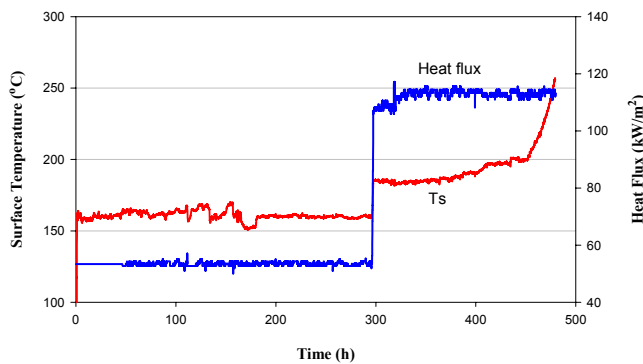


Fig. 8 Probe surface temperature (Ts) and heat flux (q) (Run 4) versus time after 86h pre-heating

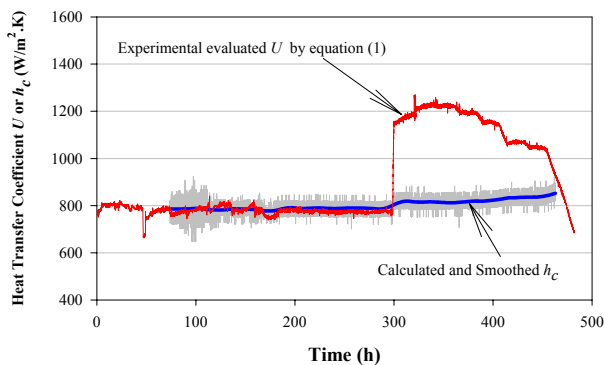


Fig. 9 Measured heat transfer coefficient U, (Run 4) and calculated convective film coefficient versus time after 86 h pre-heating

Steinhagen et al., (1986). A convective heat transfer calculation based on the Gnielinski (1975) correlation and the measured flow and thermal conditions is shown in

Figure 9. The calculated h_c values in the low heat flux regime (53kW/m^2) are close to the evaluated overall heat transfer coefficient U , indicating that heat transfer under those conditions was in the convective regime. At the high heat flux (110kW/m^2), the calculated h_c values are a factor of 1.5 lower than the measured U values, indicating that the heat transfer process has shifted to the sub-cooled flow boiling regime.

Within some 50 hours heating at 400W, the heat transfer coefficient U at about $1200\text{ W/m}^2\text{ K}$ began to decline in a series of steps, and at time about 460h a dramatic decline in heat transfer coefficient occurred, which lasted until the experiment was shut down. Figure 10 shows that the fouling rate increased in a series of steps, associated with the pressure variations for re-pressurization. The very high final fouling rate of $\sim 76 \times 10^{-7}\text{ m}^2\text{K/kJ}$, appears similar to what has previously been reported for autoxidation fouling when the solubility limit of gums has been reached (Wilson and Watkinson, 1995).

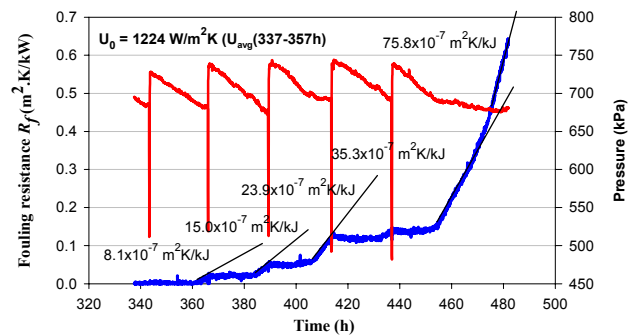


Fig. 10 Fouling resistance and pressure variations of Run 4 versus time after 86 h pre-heating

The gum content at the onset of the fouling was 2208 mg/L, and remained essentially constant at 2230 ± 20 mg/L, for the following 120h when heavy fouling occurred. The last three liquid samples (gum: 1685-2248 mg/L), appeared cloudy when they were withdrawn from the circulation system, and then separated into a clear bright yellow supernatant and a brown precipitate upon cooling to room temperature. The deposits were concentrated on the probe heated area (Figure 11a-c). A distinct layer of deposit which had formed on the probe (Figure 11b), was carefully scraped from the probe surface for further analysis.

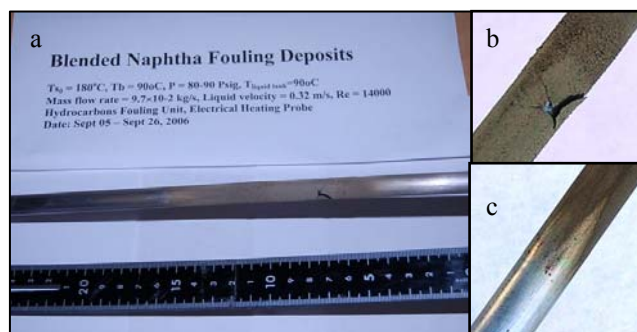


Fig. 11 Fouling deposits on heated probe surface (Run 4)

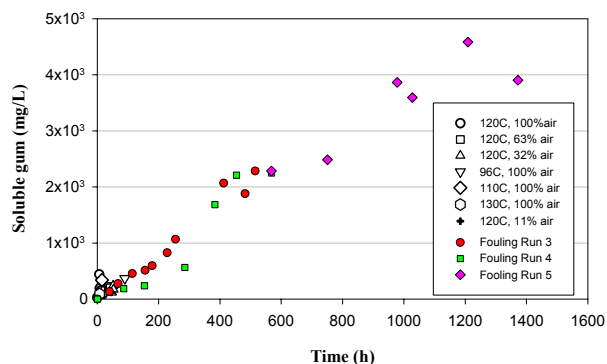


Fig. 12 Gum formation in naphtha oxidation and fouling

A subsequent experiment, Run 5, using the oxidized naphtha which was discharged from the fouling unit from Run 4 (~7L) and had been stored in the dark at room temperature for seven days. The initial gum content of the liquid was 1370 mg/L, which was 40% below that from the end of Run 4 (2248 mg/L), presumably due to settling of insoluble gum. During Run 5, four values of the heat flow were tested over 800h. Although the probe surface temperature ranged from 165°C to 215°C (Table 3), no deposition was observed. The gum contents during Run 5 increased steadily up to a level above 3000 mg/L, which is significantly higher than in the previous run (2250 mg/L)

where there was heavy fouling. The lack of fouling in Run 5 may reflect either differences in solvent composition, or the absence of the most polar and least-soluble gum constituents because of deposition during Run 4, or precipitation during storage.

Summary of Gum Formation, Composition and Thermal Properties

As the deposit precursor, gum plays an important role in the fouling process, although high dissolved gum content does not necessarily guarantee fouling. Figure 12 shows all the gum formation data. For Run 5, the gum contents and time were corrected for the initial gum loss. The data for all experiments follow a broad band of data points reaching about 4000 mg/L after about 1000h, equivalent to an average rate of roughly ~4 mg/L-h over 90-130°C.

Characterization of Gums and Deposits

Gum and deposit samples were characterized using TGA and elemental chemical analysis. Figure 13 compares the normalized % weight loss based on 110°C as a function of temperature. The onset of weight loss for all the gums occurred at about 160°C, consistent with gum measurement procedure. Significant thermal decomposition or devolatilization (~20% weight loss), occurred by 250-300°C for all the gums, including a sample (not shown) from the batch kinetic experiments. Devolatilization for the Run 4 gum samples at 286h and 384h heating, was completed at 700°C, whereas for the 568h sample the completion temperature was higher (~800°C), suggesting a more stable gum. In contrast, gum from Run 5 where no deposition occurred, was less stable, with most weight loss occurring below 500°C, and devolatilization was complete at about 650°C. The probe deposit from Run 4 was more stable than the gum, with 20% weight loss by 370°C, and completion of the devolatilization occurring only after 15 minutes at 800°C. Ash levels were essentially zero. Results of elemental (CHN) analysis are given in Table 4. All gum samples appear similar in carbon and hydrogen content, and have an average atomic ratios of H/C = 1.38, and O/C = 0.22. These ratios are consistent with the gums being mixtures of peroxides of alkyl-benzenes and alkanes (Table 1). The average H/C ratio of the deposits is 1.15, and the two values for the O/C ratio were 0.18 and 0.23. Nitrogen content of gums and deposits were below accurate detection limits (<0.3 wt %). Since no sulphur species were reported in the naphtha, oxygen was determined in the gums and deposits by difference.

Table 5 compares the results of Run 4 deposits and Run 5 gums from the pyrolysis GC/MS analysis. In pyrolysis GC/MS, the sample was heated to 675°C for 15s in helium, vaporizing and decomposing some of the organic species, generating lighter fragments. For the gum, which had not

Table 4 Elemental Analysis of Gum and Deposit Samples*

Sample	% C	% H	% O	O/C**	H/C**
Run 3-Gum-260h	71.31	8.44	20.25	0.21	1.42
Run 4-Gum-384h	70.81	7.97	21.22	0.22	1.35
Run 4-Gum-568h	70.85	8.15	21.0	0.22	1.38
Run 5-Gum-805h	70.07	7.97	21.96	0.24	1.36
Gum Avg.	70.76	8.13	21.11	0.22	1.38
Run 3-deposit	71.45	6.82	21.73	0.23	1.15
Run 4-deposit	74.70	7.13	18.17	0.18	1.15
Deposit Avg.	73.08	6.98*	19.95	0.21	1.15

* For all samples, % N are reported < 0.3 %, O calculated by difference. ** atomic ratio

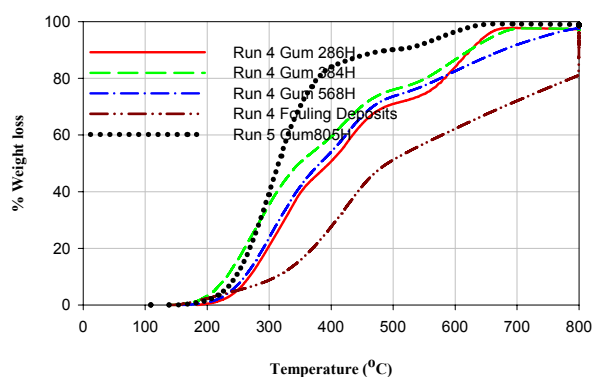


Fig. 13 Weight loss profiles of blended naphtha fouling gum and deposit TGA analysis

been exposed to the hot fouling surface, the main products of the pyrolysis are oxygenates such as ketones and acetic acid. Unsaturated fragments presumably produced by the pyrolysis, and aromatics are the other main types of species. For the deposit sample, which has been in contact with the hot metal surface, aromatics dominate, the unsaturates are much lower than for the gum, and both alkanes and cycloparaffins are present.

Table 5 Pyrolysis GC/MS Analysis of Gums and Deposits

Species	Gums-Run 5 (Area %)	Deposits-Run 4 (Area %)
CO ₂	4.0	2.7
Ketones +acetic acid	35.4	3.0 (acetone)
Light saturates (≤ C7)	5.4	23.1
Unsat'd. fragments	25.8	12.4
Aromatics	29.4	34.0
Cycloparaffins	-	10.6
Alkanes ≥ C8	-	11.3

CONCLUDING REMARKS

1. The naphtha undergoes oxidation slowly in air to produce hydroperoxides and soluble gums at temperatures in the range 96-130°C. After induction periods of 1-30 hours, peroxide concentrations rise to levels of a 1-4 meq/L, passing through a maximum over periods of 2-70h. As dissolved oxygen content is reduced from 70 to 10 ppm, the average peroxide formation rate at 120°C, decreased by an order of magnitude. The specific peroxide rate doubled with a 3.7°C rise in temperature.
2. Dissolved gum, which is a highly oxygenated material with atomic O/C ~ 0.2, appears to form in parallel, rather than in series with peroxide content. The rate of gum formation increased weakly with dissolved oxygen content, and averaged 4 -5 (mg/L)/h at about 90°C.
3. At a surface temperature of 120°C-140°C, in sensible heating (absence of boiling), no fouling was observed on the probe at gum levels reaching 2280 mg/L. Deposits were found in the dead space at the hot end of the double pipe exchanger. When at the same gum content surface temperature was raised to 180°C, resulting in sub-cooled boiling, fouling began after some 75-90h and occurred at a rapidly accelerating rate. In a subsequent test re-using the same fluid but with lower initial soluble gum, fouling was not detected over 800h, even when surface temperatures reached 215°C.
4. Gums average 21% wt. oxygen, and have H/C atomic ratios of ~ 1.38. Deposits averaged 20 % wt. oxygen, and have H/C ratios of 1.15. Aromatics appear to be more concentrated in the deposits. The gum species are highly soluble in the naphtha, reaching concentrations in excess of 2300 mg/L. The deposits appear to originate from the soluble gums, and after precipitation undergo some aging on the hot surfaces, making them thermally more stable. Deposition appears to occur only under conditions where the gum becomes highly concentrated through vaporization of the naphtha in dead zones or in sub-cooled boiling.

ACKNOWLEDGEMENTS

This work was supported by NOVA Chemicals Research and Technology Centre. Ongoing support to APW from NSERC is acknowledged.

NOMENCLATURE

A	surface area of heat transfer probe (m ²)
C _p	heat capacity at constant pressure (kJ/kg K)
E	apparent activation energy (kJ/mol)
h _c	convective film heat transfer coefficient (W/m ² K)
I	current (A)
m	mass flow rate of fluid (kg/s)
P	absolute pressure (kPa)
PO _x	peroxide concentration (mol/L)
Q	heat flow (W)
q	heat flux = Q/A; (kW/m ²)
R _f	thermal fouling resistance (m ² K/kW)
Re	Reynolds number (-)
T	temperature (°C or K)
ΔT	temperature difference T _{st} -T _b (K)
t	time (h)
t _{max}	time for peroxide rate maximum (h)
t _{in}	induction time for peroxide formation (h)
U	overall heat transfer coefficient (W/m ² K)
V	voltage (V)
v	bulk velocity (m/s)

Subscripts

b	bulk
f	fouled
max	maximum
0	clean
s	surface
st	steam
tk	tank
T	total
1	outlet end
2	inlet end

REFERENCES

Asomaning, S., Watkinson A.P., 1992, Heat Exchanger Fouling by Olefin-Kerosene Mixtures, *Can. J. Chem. Eng.*, Vol. 70, pp.444-451.

Asomaning S., Wilson D.I., Watkinson A.P., 1997, Effects of Oxygen on Fouling by Olefins in Hydrocarbon Mixtures, in *Fouling Mitigation of Industrial Heat Exchange Equipment*, CB Panchal (ed.) Begell House, New York, pp. 437-450.

Bateman L., Hughes H., Morris A.L., 1953, Hydroperoxide Decomposition in Relation to the Initiation of Radical Chain Reactions, *Disc. Faraday Soc.*, Vol. 14, pp. 190 -199.

Gnielinski, V., 1975, Neue Gleichungen für den Wärme- und Stoffübergang in turbulent durchströmten Röhren und Kanälen, *Forschung im Ingenieurwesen*, Vol. 41, No. 1, pp. 8-16.

Hess, P.S., O'Hare, G.A., 1950, Oxidation of Linseed Oil, *Ind. Eng. Chem.* Vol.42, pp.1424-1431.

Howard J.A., Ingold K.U., 1967, Absolute Rate Constants for Hydrocarbon Autoxidation: VI Alkyl Aromatics and Olefinic Hydrocarbons *Can. J. Chem.* Vol. 45, pp. 793-803.

Katta V.R., Jones E.G., Roquemore W.M., 1993, Development of Global-Chemistry Model for Jet-Fuel Thermal Stability Based on Observations from Static and Flowing Experiments, *81st Symposium, Advisory Group for Aerospace Research & Development, (AGARD) Conf. Proc. 536*, NATO, Fiuggi, Italy.

Mill T., Mayo F., Richardson, H., Irwin, K., Allara, D.L., 1972 Gas and Liquid-Phase Oxidations of Butane *J. Am. Chem. Soc.* Vol. 94:19 pp. 6802-6811.

Muller-Steinhagen, H., Watkinson, A.P., Epstein, N., 1986, Sub-cooled Boiling Heat Transfer to Heptane Flowing inside an Annulus and Past a Coiled Wire Parts 1 and 2, *J. Heat Trans.* Vol. 108, pp. 922-933.

Reich L., Stivala, S.S., 1969, *Autoxidation of Hydrocarbons and Polyolefins*, Marcel Dekker, Inc. New York.

Sajus, L., 1968, Kinetic Data on the Radical Oxidation of Petrochemical Compounds in *Adv. Chem. Ser. 75, Oxidation of Organic Compounds- Vol. 1, Chapt. 5*, pp. 59-77.

Taylor, W.F., Frankenfeld, J.W., 1986, in *Proc. 2nd Int'l Conf. on Long Term Storage Stabilities of Liquid Fuels*, L. Stavinoha (Ed.) pp. 496-511.

Taylor, W.F., 1967, Kinetics of Deposit Formation for Hydrocarbons Part 1-*IEC Prod. Res. Dev.*, Vol.6 pp.258-62, 1969, Part 3 *ibid*, Vol.8, pp. 375-80.

Wallace, T.J., 1964, Chemistry of Fuel Instability, in *Adv. Petrol. Chem. and Refining*, Vol. IX, J.J. McKetta Jr. (Ed.), Interscience, Chapter 8, pp. 353-403

Watkinson, A.P., Wilson D.I., 1997, Chemical Reaction Fouling-A Review *Experimental Thermal and Fluid Science* Vol. 14, pp. 361-374.

Wilson, D.I., Watkinson, A.P., 1995, Model Experiments of Autoxidation Fouling Parts A & B, *Trans. I. Chem. Eng.* Vol.73, pp. 59-76.

Watkinson, A.P., 2007, Deposition from Crude Oils in Heat Exchanger, *Heat Transfer Engineering*, Vol. 28, pp. 177-184.